

Low-energy excitations in multiple modulation-doped CdTe/(CdMg)Te quantum wells

D. Yavorskiy,^{1,2,3} F. Le Mardel,⁴ I. Mohelsky,⁴ M. Orlita,^{4,5} Z. Adamus,^{3,6}
T. Wojtowicz,⁶ J. Wróbel,^{3,7} K. Karpierz,⁸ and J. Łusakowski^{8,*}

¹*Institute of High Pressure Physics, PAS, ul. Sokotowska 29/37, 01-142 Warsaw, Poland*

²*CENTERA, CEZAMAT, Warsaw University of Technology, ul. Poleczki 19, 02-822 Warsaw, Poland*

³*Institute of Physics, PAS, al. Lotników 32/46, 02-668 Warsaw, Poland*

⁴*LNCMI, CNRS-UGA-UPS-INS-EMFL, 25 rue des Martyrs, 38000 Grenoble, France*

⁵*Institute of Physics, Charles University, Ke Karlovu 5, Prague, 121 16 Czech Republic*

⁶*International Research Centre MagTop, Institute of Physics,
PAS, al. Lotników 32/46, 02-668 Warsaw, Poland*

⁷*Institute of Applied Physics, Military University of Technology, Kaliskiego 2, 00-908 Warsaw, Poland*

⁸*Faculty of Physics, University of Warsaw, L. Pasteura 5, 02-093 Warsaw, Poland*

(Dated: March 31, 2025)

Low energy excitations of a two-dimensional electron gas (2DEG) in modulation-doped multiple (ten) quantum wells (QWs) was studied using far-infrared magneto-transmission technique at liquid helium temperatures. A large distance between neighbouring QWs of 54 nm excluded a direct interaction of electron wave functions confined in the wells. In four samples which differed in the spacer width and the level of doping with iodine donors, supplied with a metallic grid coupler, a uniform picture of excitations of the 2DEG was observed. These involved the cyclotron resonance (CR), its second harmonic (2CR) and magnetoplasmon modes (MPMs). MPMs with a small amplitude originated from excitations of the 2DEG in a single QW and these with a high amplitude resulted from a coherent excitation of the 2DEG in all wells. A polaron effect resulting from the interaction of the CR, 2CR and MPMs with an optical phonon was observed and described with appropriate models. Both types of MPMs exhibited gaps in the dispersion relations at the frequency close to the 2CR, leading to Bernstein modes, which was described with an appropriate (non-local) theoretical model.

I. INTRODUCTION

Low-energy excitations of a two-dimensional electron gas (2DEG) in the far-infrared (FIR, or THz frequencies) [1] have been in the focus of interest in many theoretical and experimental groups since the 1950s [2–4]. Here we report on FIR magneto-spectroscopy studies of modulation-doped CdTe/(CdMg)Te multi quantum wells (MQWs). In the response, we identify several types of FIR excitations: the cyclotron resonance (CR), its second harmonics (2CR) and magnetoplasmon modes (MPMs). In addition, we observed an interaction of the CR, 2CR and MPMs with optical phonons (a polaron effect) and gaps in the dispersion of MPMs in the region where it crosses the 2CR. The latter effect is a non-local phenomenon and mimics a truly interaction between the 2CR with MPMs. Plasma excitations in that part of MPMs spectrum are conventionally named the Bernstein modes.

The cyclotron resonance is probably the most characteristic excitation of a 2DEG subjected to the magnetic field, B , and has been widely studied because it serves as the main and precise tool to determine the single-particle effective mass. Using the quantum picture, the basic principle of the CR - an electric dipole allowed transition between subsequent Landau levels - becomes more complex when one puts it within a frame of a general de-

scription of the response of an electron gas to arbitrary electromagnetic wave [5] or one takes into account interaction between electrons and many-body effects [6–9] even though on the basic level the latter effect should not appear in systems with a strictly parabolic band [10].

This complexity have become more and more important with increased quality of samples, particularly with extreme values of the electron mobility in the case of a 2DEG. For example, in high-electron mobility GaAs-based structures one can observe nonmonotonic variations of the cyclotron effective mass with B which results (at least, partially) from filling-factor dependent screening [11] (see, however, a prior report [12]) or electron correlations observed in CR measurements which are also related to the filling factor [13]. The CR of composite fermions was observed as well [14].

A simple one-particle approach to the CR was questioned in [15, 16]. It was shown that considering the CR as a magnetoplasmon excitation, one can explain experimentally observed dependence of the CR energy on B and an absorption oscillator strength. Development of a time-resolved spectroscopy in the FIR domain (a technique referred to as THz-TDS [17]) allowed one to measure coherence times of the CR transition [18] and establish a coherent control of this transition [19]. A THz-TDS technique was also used to find out a many-body nature of decoherence of the CR in a high-electron-mobility 2DEG in GaAs QWs [20].

Magnetoplasmon modes are natural companions of the CR in a solid-state plasma in bulk materials and low-dimensional structures. They are frequently observed to-

* jerzy.lusakowski@fuw.edu.pl

gether with the CR, as it is also the case of the present paper. For a general reference on magnetoplasma effects in bulk materials, see Refs. [21, 22]. The dispersion of longitudinal waves in a 2D plasma was first considered by Stern in 1967 [23] but it took a decade for the first observation of plasmons in a 2DEG to be reported in [24]. Theoretical analysis of Stern was further developed by Greene [5] and Chiu and Quinn [25] to include the magnetic field.

In the last two decades, new directions of research of magnetoplasmons have been opened and have become dominated by studies of plasmons in graphene [26–31] and field-effect transistors [32–37]. A particularly interesting junction of subjects: graphene, plasmons and a near-field nanoscopy can be found, e.g., in [38]. Let us note that a large part of all these contemporary studies, although originating and tightly bound to fundamental physics, are devoted to applications of plasmonic devices as detectors or emitters of FIR radiation. For an older and a recent review devoted to the electron plasma in two dimensions in solids, see [39] and [40], respectively.

Cadmium telluride is a semiconductor with a strong electron - phonon interaction which facilitates the observation of polaronic effects. The papers [41] and [42] are among the first theoretical approaches to the polaron theory. Some further contributions to the theory of the polaron effect was presented by, e.g., Peeters and Devreese [43] and Pfeffer and Zawadzki [44, 45]. A valuable recent review on the polaron effect is given in [46] - it contains a detailed account on the history of development of the theory of polarons and a broad list of references to theoretical and experimental works. An account on earlier studies can be found in [47].

Very often, the polaron effect is observed as an increase of the cyclotron electron effective mass when the energy of the CR transition is close to that of the optical phonon [48] as it was observed in a single CdTe/(CdMg)Te QW in a previous publication [49]. However, optical phonons can interact also with magnetoplasmons and the study of interaction between (magneto)plasmons and optical phonons is another broad area of research in solids. Theoretically, in the case of a degenerate statistics, this interaction was first described by Yokota [50], Varga [51] and Lee and Tzoar [52] and then observed by Mooradian and Wright [53]. Dispersion of plasmon-phonon polaritons can be determined by Raman scattering, which is the most widely used technique in such studies, or by photoluminescence which is particularly useful in the case of magnetoplasmons (see, e.g., [54] and [55], respectively, reporting results on bulk semiconductors). The interaction of plasmons with optical phonons in two-dimensional systems is considered theoretically in many papers (e.g., for a graphene-oriented review, see [56]) but not many experimental results have been so far presented for a 2DEG in semiconductor QWs [57].

The present paper shows a strongly polar 2D semiconductor system in which such an interaction can be ob-

served. A conclusion which results from our phenomenological analysis of the polaron effect in samples studied is that a quantitative description of this effect, which is in our case defined by the frequency ω_{ph} of a phonon taking part in the polaron interaction, seems to depend on the sample. Tentatively, we attribute this effect to sample-dependent disorder of the layers adjacent to the QWs.

Derivation of the dispersion relation of the plasma oscillations requires an approach in which one first determines the conductivity tensor of the plasma and then uses it to solve the Maxwell's equations. Generally, this leads to the plasma dispersion relation which is non-local, i.e., next to an explicit dependence on the plasmon wave vector it also depends on the product of the wave vector k and the cyclotron radius r_c . Following this procedure, Bernstein showed [21] that at given magnetic field, the gaps open at frequencies near the harmonics of the CR. Thus, when the frequency of a MPM approaches that of a CR harmonic, an avoided crossing appears in the MP dispersion. This phenomenon attracted attention of researchers and was studied in a large number of papers, both theoretical and experimental, an exemplary account of which are given by [55, 58–70].

Traditionally, the parts of the non-local plasmon dispersion which are situated in the vicinity of the harmonics of the CR are called the Bernstein modes. As it is clearly shown, e.g., in Ref. [25, 70], the upper hybrid mode is composed of these parts of the dispersion relation for which non-local corrections are negligible and the dispersion can be very well approximated by the local approach. It follows that a division of the MP dispersion to the upper hybrid mode and Bernstein modes is artificial and particularly misleading when these two notions are confronted as entities of a different origin. However, for brevity and following the tradition, we will use in the following the notion "Bernstein modes" by which we will mean just a part of the dispersion in the vicinity of the harmonics of the CR. We will come back to an analysis of the non-local dispersion relation in Section IV. As a perfect introduction to the local theory of plasma waves, we recommend in addition to [22] also introductory chapters of [71].

Interestingly, the Bernstein modes have so far been studied almost exclusively in bulk GaAs and GaAs-based low dimensional structures. One of the first observations of Bernstein modes in other solid-state systems, GaN/(AlGa)N heterostructures, was reported in [72] which was followed by a recent observation in graphene [73]. The present paper presents an analysis of Bernstein modes in CdTe/(CdMg)Te MQWs. Here, according to our interpretation, the gaps in the dispersion relation open in the case of plasmons excited in a single QW and coherently in all ten QWs. The former type of Bernstein modes has not yet been observed, to the best of our knowledge.

The present paper considers results of a FIR Fourier transmission spectroscopy of CdTe/(CdMg)Te MQWs.

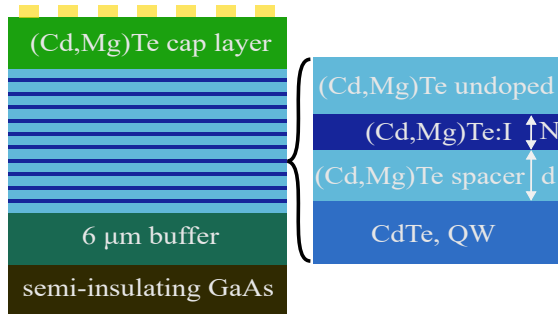


FIG. 1: A scheme of samples' structure (not to scale). One period of the active part of the sample is enlarged to show the sequence of the layers and indicate the meaning of parameters d and N .

The case of single QWs was considered in [49, 74] where one can find a referenced summary on previous studies on the CR in CdTe/(CdMg)Te single QWs.

The paper is organized as the following. Section II describes the samples used and the experimental system. Results of measurements are presented in Section III and discussed in Section IV. Then we conclude the paper.

II. EXPERIMENTAL

The samples studied were grown by the molecular beam epitaxy on a semi-insulating GaAs substrate and contained ten QWs. In each case, the QWs were grown from CdTe while barriers were always a mixed crystal $\text{Cd}_{0.7}\text{Mg}_{0.3}\text{Te}$. All QWs in a given sample were nominally identical - their width, the thickness of the spacer d and the doping was the same (doping was introduced after a QW was grown). The level of doping is described by the number of monolayers (N) in which iodine donors were introduced. The temperature of the iodine source was the same during the growth of all doped layers in all samples which allows us to assume that the concentration of donors in a doped region is the same. The samples differed by N and d . The distance between subsequent QWs is equal to 54 nm which allows us to consider them as non-interacting in the sense that electron's wave functions from neighbouring wells do not overlap. However, interaction with FIR radiation which leads to a collective excitation of all QWs in the sample is evidenced by experimental data, as it will be shown further on.

A scheme of samples' structure is shown in Fig. 1. Parameters of the samples are given in Table I; the last column shows the value of the electron effective mass (in units of the free electron mass, m_e) determined from the CR by a Fourier spectroscopy to be described further on; the relative error of m^* is equal to about 10^{-3} . The values of concentration n (per well) presented in Table I are obtained from fitting of magnetoplasmon dispersions, which is explained in Section IV. As one can notice, these values of n change with technological parameters d and

N as expected (i.e., the thinner spacer and the wider doped layer, the higher the electron concentration).

Two sets of samples were studied: one set contained as grown samples and the other - samples with a lithographically prepared metallic (Cr/Au) 50 nm-thick grid on their surface. In all cases, the period of the grid was $2 \mu\text{m}$ with $\alpha = 0.5$ of the geometrical aspect ratio.

TABLE I: Samples' parameters

Sample	d [nm]	N	n [cm^{-2}]	m^* [m_e]
MQW ₁	5	12	1.10×10^{12}	0.103
MQW ₂	10	12	1.07×10^{12}	0.103
MQW ₃	20	12	9.61×10^{11}	0.101
MQW ₄	20	9	8.69×10^{11}	0.100

The samples were placed in the center of a 16 T coil and cooled in dark to 4.2 K with helium exchange gas at low pressure. No additional near-band-gap illumination during measurements was used. Transmission spectra were registered with a Fourier spectrometer as a function of B with a bolometer placed below the sample. The spectra were registered at selected values of B each 0.25 T with the resolution of about 1.0 cm^{-1} .

A graphical presentation of the procedure of numerical data treatment is presented in Fig. 2 for spectra measured at 12 T on MQW₁ and GMQW₁ (the letter G stands for the grid). The raw data (black dots in Fig. 2) were first numerically filtered to remove Fabry-Perot interferences. As a normalization procedure, we chose to divide each filtered spectrum by a mean spectrum which was obtained as the arithmetic average of all filtered spectra measured for given sample in the whole range of B (solid black line in Fig. 2). The results are shown as green and red solid lines. This allowed us to determine positions of the main spectral features, i.e., the CR and MPs, as is indicated by arrows in Fig. 2. However, to analyze spectral features that are weaker in their intensity, it was necessary to construct color maps showing a derivative of the signal with respect to the magnetic field (by the derivative we mean a difference of two spectra measured at B differed by 0.25 T; in calculating the derivative, we used spectra after filtering-out Fabry-Perot interferences but not normalized). The high-energy cut-off of the data presented at about 140 cm^{-1} is defined by the Reststrahlen band of CdTe.

III. RESULTS

Figure 3 shows results measured on MQW samples without a grid. The dotted red lines show the expected ($\hbar e B / m^*$) first and the second harmonics of the CR. There are two clearly visible features: a small deviation from the linearity caused by the polaron effect in the case of the CR and a much stronger polaron interaction in the case of the 2CR.

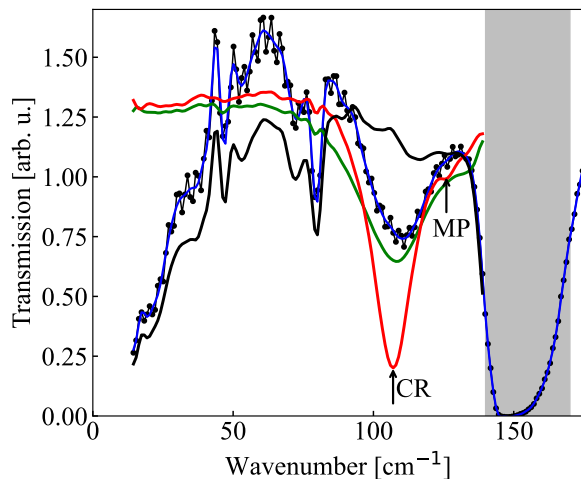


FIG. 2: Black dots: the raw spectrum measured on MQW₁ at 12 T. Blue: the same spectrum after removing Fabry-Perot interferences. Solid black: a mean spectrum. Solid green: the blue spectrum after normalization with the mean spectrum. Solid red: the result of treatment of a spectrum measured at 12 T on GMQW₁. The arrows show positions of the cyclotron resonance (CR - the same for the green and red spectra) and the magnetoplasmon (MP, present in GMQW₁ only). The grey rectangle shows the Reststrahlen band of CdTe, between 140 and 170 cm⁻¹.

Transmission results on samples with a grid are presented in Fig. 4. As compared to Fig. 3, the samples with a grid display considerably richer behaviour. First, the interaction of the 2CR with an optical phonon is less pronounced, however, an additional feature emerges - gaps in the magnetoplasmon dispersion which are clearly visible in areas indicated by the red circles. Second, there is a strong MPM with the energy about 80 cm⁻¹ at $B = 0$ which also interacts with the optical phonon. This interaction leads to a bending of the MPM towards the CR line. Lower-energy MPMs are well visible in the case of GMQW₂ sample, although they could be also detected in the data of other samples under a careful inspection.

To compare experimental results with a theoretical model, we present in Fig. 5 the positions of the above mentioned spectral features.

IV. DISCUSSION

A. The second harmonics of the CR and polaron interactions

For a uniform system, electric-dipole allowed optical transitions between Landau levels (LLs) are possible only between pairs of adjacent LLs. The second or higher harmonics of the CR were observed in some optical FIR or microwave experiments [75–78] but no consistent pic-

ture of conditions at which the 2CR may appear has so far been established. Generally, one can expect that symmetry-breaking mechanisms must be involved like a strong scattering, electric field or non-parabolicity.

Particularly appealing theoretical models were proposed in [79, 80] which relate excitation of the CR harmonics to a strong electric field generated by the incoming electromagnetic wave on edges of metallic elements (ohmic contacts, gates, grids) present on the sample's surface. However, our data seem to show just the opposite: the 2CR in samples with the grid is much weaker than in samples without it. This means that other symmetry-breaking mechanism should be invoked.

In the case of samples studied here, the 2CR itself is not only clearly visible in the data but also exhibits evidence of interaction with MPMs (blue and green dots in Fig. 5) and the optical phonon (red points in Fig. 5).

CdTe is a material with a strong interaction of electrons with optical phonons. This is expressed by a high value of the Fröhlich constant equal to 0.286 [81]. The polaron effect was observed in single CdTe/(CdMg)Te QWs in the past [74, 82, 83] as a deviation from a linear dependence of the CR transition at high B . Here, the polaron interaction is manifested via B -dependence of the CR, 2CR as well as on MPMs.

To describe the interaction of the CR and 2CR with optical phonons, we apply a phenomenological approach based on a Hamiltonian \hat{H} of a two-level system with an interaction described by Ω_i :

$$\hat{H} = \hbar \begin{bmatrix} \omega_i & \Omega_i \\ \Omega_i^* & \omega_{ph} \end{bmatrix}. \quad (1)$$

The above Hamiltonian describes interaction of two oscillators: a CR-related oscillator (with $i = 1$ or 2 corresponding to the CR or 2CR, respectively) with the frequency $\omega_i = ieB/m^*$ and an optical phonon with the frequency ω_{ph} . The energy of interacting levels is then given by

$$E_i = \frac{\hbar}{2} \left(\omega_i + \omega_{ph} \pm \sqrt{(\omega_i - \omega_{ph})^2 + 4|\Omega_i|^2} \right) \quad (2)$$

We fitted the lower energy solution to experimental values of the 2CR frequency dependence on B in the case of samples without and with the grid obtaining mean values of $|\Omega|_{2CR}$ and ω_{ph} . Next, the extracted parameters ω_{ph} were used to obtain the values of $|\Omega|_{CR}$ describing the polaron interaction in the case of the first harmonic. Results of the fitting are presented in Table II while the dependencies resulting from the fitting are shown as red dashed lines in Fig. 5. This figure shows also the Reststrahlen band of CdTe and the energy of phonons determined by fitting. The Ockham's razor allows us to assume that both the CR and 2CR are influenced by the same phonon, but this does not necessarily need to be the case.

The presence of interfaces modifies energies of phonons known from studies of bulk materials. First, there are

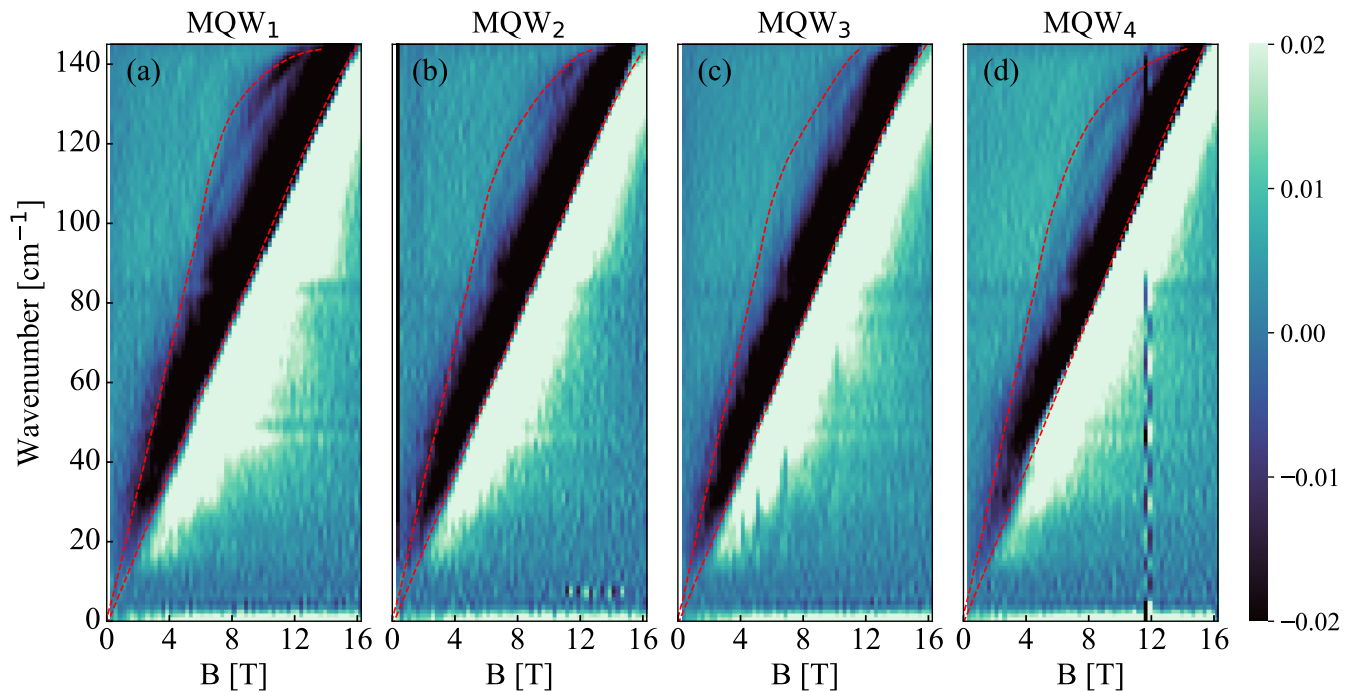


FIG. 3: Transmission data on MQW₁- MQW₄ samples (a) - (d), respectively. Thin red dotted lines show the CR and the 2CR.

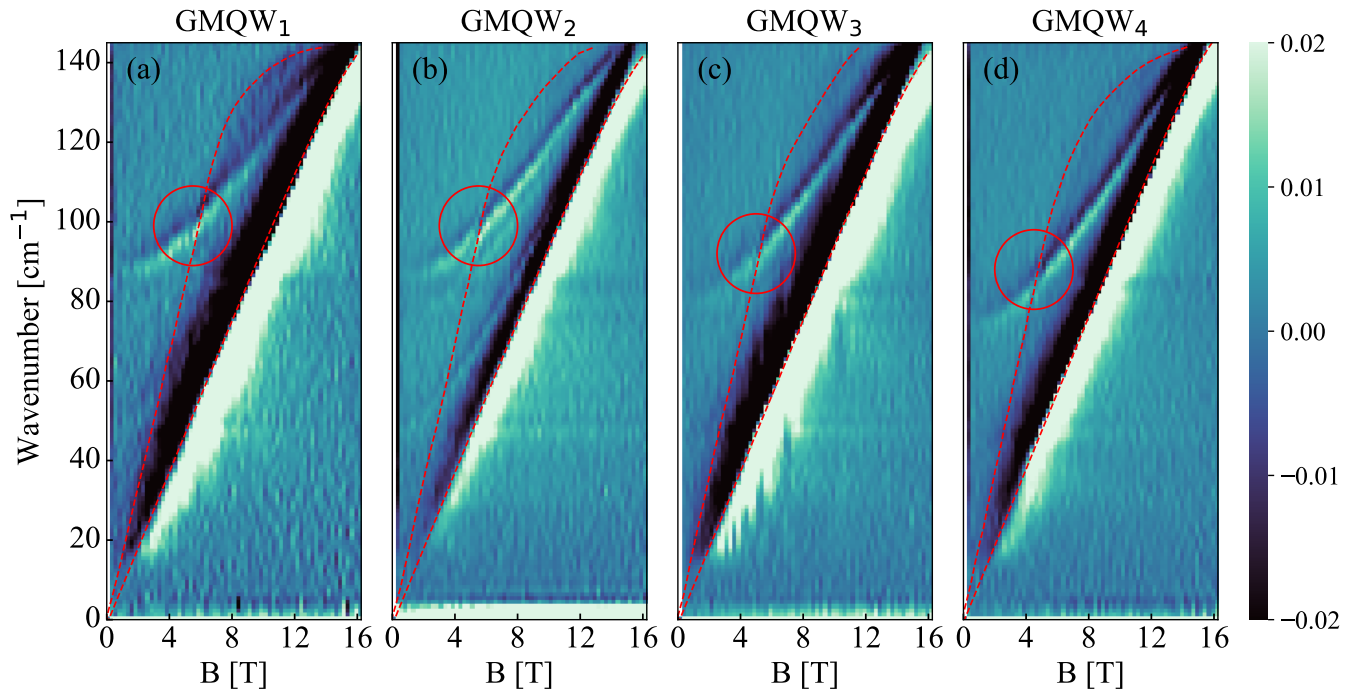


FIG. 4: Transmission data on GMQW₁ - GMQW₄ samples (a) - (d), respectively. The red circle shows the region of Bernstein modes.

phonons propagating in the proximity of interfaces, which are absent in bulk materials: these vibrations involve different sets of atoms than in bulk which changes their fre-

quency. Such interface-related phonons are particularly important in the case when the polaron interaction involves a 2DEG residing in a proximity of the interface.

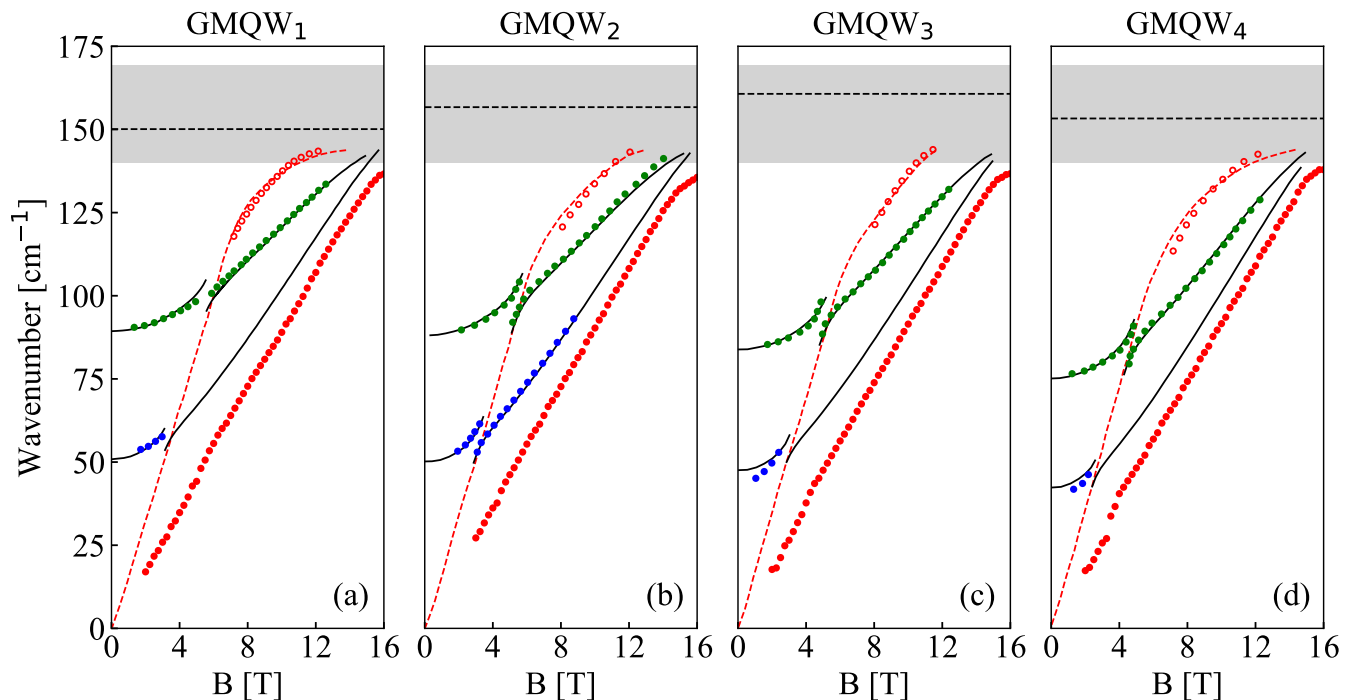


FIG. 5: Red solid dots: CR with interaction with an optical phonon. Red open dots: 2CR with interaction with an optical phonon. Red dashed lines: results of fitting of Eq. 1. Blue dots: a low-energy magnetoplasmon with interaction with 2CR. Green dots: a high-energy magnetoplasmon with interaction with 2CR. Black lines: calculated magnetoplasmon energy according to Eq. 3. Grey rectangle - the CdTe Reststrahlen band. Dashed lines - fitted energy of phonons ω_{ph} from Table II.

Second factor, especially important in a strongly polar material such as CdTe, is due to modification of electron-phonon interaction resulting from localization of electron wave function in QWs which changes efficiency of screening. For a general reference on this subject we recommend Ref. [84] and Ref. [85, 86] specifically devoted to studies of phonons in CdTe-based nanostructures. Photoluminescence spectra with phonon replicas and Raman scattering spectra obtained on MQW₂ sample were presented in [87]. It was shown that the frequency of optical phonons which result from such processes were shifted with respect to values obtained in studies on bulk CdTe. For these reasons, we do not specify the nature of the phonon which interacts with the CR and 2CR. A final identification should be based on more complete Raman scattering - oriented studies on these samples which is beyond the scope of the present paper.

Landolt-Börnstein data base [88] reports values of a transverse optical phonon in CdTe between 141 and 146 cm^{-1} . Analyzing the values of ω_{ph} we notice that at the constant $N = 12$ there is a systematic shift to higher frequencies with increasing d but then a rapid decrease for the smallest doping (the largest d and the lowest N , sample $l=4$). Also, we note that the polaron effect on the 2CR is essentially stronger than in the case of the CR. This can be observed directly in experimental data where bending of the 2CR line occurs at much lower B

than in the case of the CR. This fact is reflected in the value of the interaction constant $|\Omega|_{2CR}$ which is clearly larger than $|\Omega|_{CR}$.

At the moment, we cannot give a definitive interpretation of this difference. However, if the strength of the interaction is to be estimated on the basis of a deviation of the CR (or 2CR) vs B dependence from the straight line, then we may refer to Fig. 2b in Ref. [49] which shows the polaron effect on the CR in a single CdTe/(CdMg)Te QW with parameters very similar to these of QWs studied here. The polaron effect there observed starts to be visible at about 10 T and is essentially stronger than that observed in the present study, where it is visible only at the highest B about 14 T. The conclusion is that the polaron effect in the CR in CdTe/(CdMg)Te QWs is apparently very sensitive to microscopic details of the QWs studied. This could be related to the disorder of the layers or interfaces adjacent to the QW modifying the spectrum of phonons interacting with electrons in the QWs. Different phonon frequencies ω_{ph} obtained from fitting suggest that these values are sample-specific which could support this disorder - related interpretation.

TABLE II: Polaron interaction - average values from MQW_l and GMQW_l samples; $l = 1, \dots, 4$

l	d [nm]	Doping [ML]	$\hbar \Omega _{CR}$ [cm ⁻¹]	$\hbar \Omega _{2CR}$ [cm ⁻¹]	ω_{ph} [cm ⁻¹]
1	5	12	1.68 ± 0.03	3.15 ± 0.07	150.1 ± 0.6
2	10	12	1.70 ± 0.03	4.22 ± 0.12	156.7 ± 1.3
3	20	12	1.58 ± 0.05	4.22 ± 0.05	160.7 ± 0.6
4	20	9	1.26 ± 0.06	3.79 ± 0.08	153.3 ± 0.8

B. Magnetoplasmon modes

Magnetoplasmon modes are clearly visible in data presented in Fig. 4 and their dispersion exhibits two features. The first one is an avoided crossing at the energy where the magnetoplasmon dispersion coincides with the 2CR transition, which is traditionally referred to as Bernstein modes, as it was explained in Introduction. The second one is bending of the magnetoplasmon dispersion resulting from interaction of magnetoplasmons with the optical phonon. Both interactions can be modeled with the dispersion relation given by:

$$\frac{\omega^2 - \omega_{LO}^2}{\omega^2 - \omega_{TO}^2} - \frac{\omega_{p,j}^2}{X_j^2} \sum_{l=1}^{\infty} \frac{4l^2 J_l^2(X_j)}{\omega^2 - (l\omega_c)^2} = 0, \quad (3)$$

where $\omega_{p,j}$ and k_j is the frequency and the wave vector of j^{th} plasmon mode at $B = 0$, respectively:

$$\omega_{p,j} = \sqrt{\frac{e^2 n k_j}{2m^* \epsilon_0 \epsilon_{\text{eff}}}}, \quad (4)$$

and $X_j = k_j r_c$ where r_c is the cyclotron radius. For derivation of Eq. 3 see [74] and references therein; for short - this formula involves polarization of the system coming from the lattice (the first term) and from a non-local effect in the electron gas (the second term).

In the analysis of the dispersion relation we are interested in the long-wavelength limit with $X_j \ll 1$. Results of numerical calculations of the dispersion relation resulting from the second term in Eq. 3 are shown in [70] while a discussion of analytical expressions is presented in [25], Sec. IVA. Following the latter reference, one can show that if ω/ω_c is not too close to 2 (and also to any integer greater than 2), then the dispersion relation resulting from Eq. 3 coincides with that based on local classical considerations, i.e., with the upper hybrid mode. A further analysis of the dispersion at ω/ω_c close to any integer equal or greater than 2 shows that the dispersion splits and the gaps in the dispersion open what is shown by numerical calculations in [70].

The effective dielectric function ϵ_{eff} is different for gated and ungated plasmons. In the case of a grid-gated samples, one deals with a partially gated surface. In previous publications, where magnetoplasmons were studied in grid-gated samples of CdTe/(CdMg)Te QWs (Ref. 74), GaAs/(GaAl)As (Ref. 77) and GaN/(GaAl)N (Ref. 72)

heterostructures, we found that the frequency of magnetoplasmon resonances were very well reproduced if one took a weighted average of dielectric functions of gated (ϵ_g) and ungated (ϵ_{ug}) plasmons and used a geometrical factor (α) describing the percentage of surface covered with the metal to obtain $\epsilon_{\text{eff}} = \alpha\epsilon_g + (1 - \alpha)\epsilon_{ug}$. In this formula, $\epsilon_g = 1/2[\epsilon_s + \epsilon_b \coth(k_j d)]$ and $\epsilon_{ug} = 1/2[\epsilon_s + \epsilon_b(1 + \epsilon_b \tanh(k_j d))/(\epsilon_b + \tanh(k_j d))]$ [89], where ϵ_s and ϵ_b are dielectric constants of the QW and the barrier, respectively.

Solutions of Eq. 3 are shown as black lines in Fig. 5. The fitting procedure leading to these dependencies started with the electron effective mass determined from the CR shown in Fig. 3 taking the data between 6 and 12 T only to avoid the noise in the signal at low- B and the polaron interaction at the highest B . The values of the dielectric constant of CdTe (equal to 7.1) and that of (CdMg)Te (equal to 5.9) as well as optical phonons ($\omega_{TO} = 140.1 \text{ cm}^{-1}$ and $\omega_{LO} = 169.45 \text{ cm}^{-1}$) were the same as used in [74].

As evident from the above description, the dispersion of magnetoplasmons involves many parameters and one has to decide which one is the best to reproduce the experimental data theoretically. There are two natural candidates: the effective dielectric constant and the electron concentration. As we explained above, we verified on different semiconducting systems the validity of using the effective dielectric constant in the form of a weighted average of constants of gated and ungated plasmons. Therefore, in this study we follow this approach and we choose the electron concentration as a fitting parameter.

There are two MPMs clearly visible for each data set presented in Fig. 5 (blue and green symbols) with the higher-energy mode stronger as compared to the lower-energy one. As a starting point for the fitting, we used results of our magneto-transport experiments (not presented in this paper) which allowed us to estimate a 2DEG concentration in each sample. Then we plotted $\omega_{p,j}$ for plasmonic modes, numbered by j , propagating in a single QW. It appeared that in each sample the low-frequency mode nearly coincided with $j=2$ plasmonic mode in a single QW. At this point, the electron concentration was finally adjusted to reproduce the data with the dispersion of $j=2$ mode. The resulting concentrations are presented in Table I. As we mentioned above, a close inspection of the data allows one to find weak signatures of the fundamental $j=1$ mode. Having identified the low-frequency mode, we found that the other one

corresponds to a fundamental mode of a system which can be described as a single QW but with the electron concentration ten times higher than in a corresponding single QW. Thus, we conclude that there are arguments showing that the high-frequency mode results from a coupled response of all QWs in the sample. A high intensity of this mode supports this interpretation.

On the other hand, we would like to point out that the above conclusion is an experimental one and requires a theoretical support coupled to yet another type of experiment, e.g., Raman scattering. Electrodynamics of a layered electron gas was considered first by Fetter [90, 91] then by other authors (see, for example [92–94]) and numerical simulations were presented by Aleshkin and Dubinov [95]. Experimentally, the plasma dispersion was studied in such systems by inelastic light scattering [96, 97]. The theory predicts that the layered 2DEG behaves as a 2D system for large separation of the QWs, i.e., when $kd \gg 1$, otherwise its dispersion tends to that of a bulk material. In our case, the wave vector, defined by the period of the grid is $k = 2\pi/2 \mu\text{m}^{-1}$, $d \approx 50 \text{ nm}$ and $kd \approx 0.15$ which is on the border between these two cases. Thus we put off the final conclusions on the nature of the strong magnetoplasmon mode until Raman scattering experiments will have been performed.

The polaron interaction of MPMs is less pronounced as compared to the case of the CR and 2CR although experimental points follow well the dependence given by Eq. 3 (black lines in Fig. 5). The reason for the absence of a clear bending of this dispersion comes from the fact that magnetoplasmons interact with longitudinal optical phonons which frequency is about 170 cm^{-1} [88] and is far above the range of energy where magnetoplasmon modes were presented in Fig. 4.

V. CONCLUSIONS

In conclusion, multiple CdTe/(CdMg)Te modulation-doped QWs proved to be a semiconducting system which allows one to observe a series of low-energy excitations of a 2DEG in a single magneto-spectroscopy experiment.

These include: the CR with its second harmonic, magnetoplasmons and interaction of these excitations with optical phonons showing the polaron effect. Also, the gaps in the dispersion of MPMs leading to the Bernstein modes, were observed in CdTe-based structure for the first time. A particularly interesting observation was a high-amplitude MPM which was interpreted as resulting from a coherent excitations of oscillations of the electron plasma in all ten QWs. The Bernstein modes were observed also for this coherent mode (for the first time, to the best of our knowledge) which underlines the validity of a general non-local description of plasma excitations.

ACKNOWLEDGMENTS

This research was partially supported by the Polish National Centre grant UMO-2019/33/B/ST7/02858 by the “MagTop” project (FENG.02.01-IP.05-0028/23) carried out within the “International Research Agendas” programme of the Foundation for Polish Science co-financed by the European Union under the European Funds for Smart Economy 2021-2027 (FENG). Publication subsidized from the state budget within the framework of the programme of the Minister of Science (Polska) called Polish Metrology II project no. PM-II/SP/0012/2024/02, amount of subsidy 944,900.00 PLN, total value of the project 944,900.00 PLN.

The work was supported by the European Union through ERC-ADVANCED grant TERAPLASM (No. 101053716). Views and opinions expressed are, however, those of the author(s) only and do not necessarily reflect those of the European Union or the European Research Council Executive Agency. Neither the European Union nor the granting authority can be held responsible for them. We also acknowledge the support of "Center for Terahertz Research and Applications (CENTERA2)" project (FENG.02.01-IP.05-T004/23) carried out within the "International Research Agendas" program of the Foundation for Polish Science co-financed by the European Union under European Funds for a Smart Economy Programme.

The analysis of magnetotransport data by E. Imos is also acknowledged.

-
- [1] We limit our interest here to a FIR part of the electromagnetic spectrum although excitations of a 2DEG with microwaves are also of a vivid interest - see, e.g., I. A. Dmitriev, A. D. Mirlin, D. G. Polyakov, and M. A. Zudov, Nonequilibrium phenomena in high Landau levels Rev. Mod. Phys. **84**, 1709 (2012).
 - [2] G. Dresselhaus, A. F. Kip, and C. Kittel, Cyclotron resonance of electrons and holes in silicon and germanium crystals, Phys. Rev. **98**, 368 (1955).
 - [3] J. M. Luttinger, Quantum theory of cyclotron resonance in semiconductors: General theory, Phys. Rev. **102**, 1030 (1956).
 - [4] G. Abstreiter, J. P. Kotthaus, and J. F. Koch, Cyclotron resonance of electrons in surface space-charge layers on silicon, Phys. Rev. B **14**, 2480 (1976).
 - [5] M. P. Greene, H. J. Lee, J. J. Quinn, and S. Rodriguez, Linear response theory for a degenerate electron gas in a strong magnetic field, Phys. Rev. **177**, 1019 (1969).
 - [6] Z. Schlesinger, S. J. Allen, J. C. M. Hwang, P. M. Platzman, and N. Tzoar, Cyclotron resonance in two dimensions, Phys. Rev. B Rapid Comm. **30**, 435 (1984).
 - [7] C. Kallin and B. I. Halperin, Excitations from a filled Landau level in the two-dimensional electron gas, Phys. Rev. B **30**, 5655 (1984).

- [8] C. Kallin and B. I. Halperin, Many-body effects on the cyclotron resonance in a two-dimensional electron gas, *Phys. Rev. B* **31**, 3635 (1985).
- [9] A. H. MacDonald and C. Kallin, Cyclotron resonance in two dimensions: electron-electron interaction and band nonparabolicity, *Phys. Rev. B* **40**, 5795 (1989).
- [10] W. Kohn, Cyclotron Resonance and de Haas-van Alphen Oscillations of an Interacting Electron Gas, *Phys. Rev.* **123**, 1242 (1961).
- [11] E. Batke, H. L. Störmer, A. C. Gossards, and J. H. English, Filling-factor-dependent cyclotron mass in space-charge layers on GaAs, *Phys. Rev. B* **37**, 3093 (1988).
- [12] T. K. Lee and J. J. Quinn, Quantum oscillations in screening in a two-dimensional electron gas, *Surface Science* **8**, 148 (1976).
- [13] M. Manger, E. Batke, R. Hey, K. J. Friedland, K. Köhler, and P. Ganser, Filling-factor-dependent electron correlations observed in cyclotron resonance, *Phys. Rev. B* **63**, 121203(R) (2001).
- [14] I. V. Kukushkin, J. M. Smet, K. von Klitzing, and W. Wegscheider, Cyclotron resonance of composite fermions, *Science* **415**, 409 (2002).
- [15] Y. A. Bychkov and G. Martinez, Magnetoplasmon and cyclotron resonance in a two-dimensional electron gas, *Phys. Rev. B* **72**, 195328 (2005).
- [16] C. Faugeras, G. Martinez, A. Riedel, R. Hey, K. J. Friedland, and Y. Bychkov, Evidence for magnetoplasmon character of the cyclotron resonance response of a two-dimensional electron gas, *Phys. Rev. B* **75**, 035334 (2007).
- [17] J. Neu and C. A. Schmuttenmaer, Tutorial: An introduction to terahertz time domain spectroscopy (thz-tds), *J. Appl. Phys.* **124**, 231101 (2018).
- [18] X. Wang, D. J. Hilton, J. L. Reno, D. M. Mittleman, and J. Kono, Direct measurement of cyclotron coherence times of high-mobility two-dimensional electron gases, *Optics Express* **18**, 12354 (2010).
- [19] T. Arikawa, X. Wang, D. J. Hilton, J. L. Reno, W. Pan, and J. Kono, Quantum control of a Landau-quantized two-dimensional electron gas in a GaAs quantum well using coherent terahertz pulses, *Phys. Rev. B* **84**, 241307(R) (2011).
- [20] A. Zhang, T. Arikawa, E. Kato, J. L. Reno, W. Pan, J. D. Watson, M. J. Manfra, M. A. Zudov, M. Tokman, M. Erukhimova, A. Belyanina, and J. Kono, Superradiant decay of cyclotron resonance of two-dimensional electron gases, *Phys. Rev. Lett.* **113**, 047601 (2014).
- [21] I. B. Bernstein, Waves in a Plasma in a Magnetic Field, *Phys. Rev.* **109**, 10 (1958).
- [22] E. D. Palik and J. K. Furdyna, Infrared and microwave magnetoplasma effects in semiconductors, *Rep. Prog. Phys.* **33**, 1193 (1970).
- [23] F. Stern, Polarizability of a two-dimensional electron gas, *Phys. Rev. Lett.* **18**, 546 (1967).
- [24] S. J. Allen, D. C. Tsui, and R. A. Logan, Observation of the two-dimensional plasmon in silicon inversion layers, *Phys. Rev. Lett.* **38**, 980 (1977).
- [25] K. W. Chiu and J. J. Quinn, Plasma oscillations of a two-dimensional electron gas in a strong magnetic field, *Phys. Rev. B* **9**, 4724 (1974).
- [26] F. H. L. Koppens, D. E. Chang, and F. J. G. de Abajo, Graphene plasmonics: A platform for strong light-matter interaction, *Nano Letters* **11**, 3370 (2011).
- [27] I. Crassee, M. Orlita, M. Potemski, A. L. Walter, M. Ostler, T. Seyller, I. Gaponenko, J. Chen, and A. B. Kuzmenko, Intrinsic terahertz plasmons and magnetoplasmons in large scale monolayer graphene, *Nano Letters* **12**, 2470 (2012).
- [28] A. N. Grigorenko, M. Polini, and K. S. Novoselov, Graphene plasmonics, *Nature Photonics* **6**, 749 (2012).
- [29] G. X. Ni, A. S. McLeod, Z. Sun, L. Wang, L. Xiong, K. W. Post, S. S. Sun, B.-Y. Jiang, J. Hone, C. R. Dean, M. Fogler, and D. N. Basov, Fundamental limits to graphene plasmonics, *Nature* **577**, 530 (2018).
- [30] L. Xiong, C. Forsythe, M. Jung, A. S. McLeod, S. S. Sun, Y. M. Shao, G. X. Ni, A. J. Sternbach, S. Liu, J. H. Edgar, E. J. Mele, M. M. Fogler, G. Shvets, C. R. Dean, and D. N. Basov, Photonic crystals for graphene plasmons, *Nature Comm.* **10**, 4780 (2019).
- [31] M. Kravtsov, A. L. Shilov, Y. Yang, T. Pryadilin, M. A. Kashchenko, O. Popova, M. Titova, D. Voropaev, Y. Wang, K. Shein, I. Gayduchenko, G. N. Goltsman, M. Lukianov, A. Kudriashov, T. Taniguchi, K. Watanabe, D. A. Svintsov, S. Adam, K. S. Novoselov, A. Principi, and D. A. Bandurin, Viscous terahertz photoconductivity of hydrodynamic electrons in graphene, *Nature Nanotechnology* (2024).
- [32] M. Dyakonov and M. S. Shur, Shallow water analogy for a ballistic field effect transistor: new mechanism of plasma wave generation by dc current, *Phys. Rev. Lett.* **71**, 2465 (1993).
- [33] L. Vicarelli, M. S. Vitiello, D. Coquillat, A. Lombardo, A. C. Ferrari, W. Knap, M. Polini, V. Pellegrini, and A. Tredicucci, Graphene field-effect transistors as room-temperature terahertz detectors, *Nature Materials* **11**, 865 (2012).
- [34] W. Knap, S. Rumyantsev, M. S. Vitiello, D. Coquillat, S. Blin, N. Dyakonova, M. Shur, F. Teppe, A. Tredicucci, and T. Nagatsuma, Nanometer size field effect transistors for terahertz detectors, *Nanotechnology* **24**, 214002 (2013).
- [35] V. Ryzhii, C. Tang, T. Otsuji, M. Ryzhii, V. Mitin, and M. S. Shur, Resonant plasmonic detection of terahertz radiation in field-effect transistors with the graphene channel and the black-As_xP_{1-x} gate layer, *Scientific Reports* **13**, 9665 (2023).
- [36] G. R. Aizin, S. Mundaganur, A. Mundaganur, and J. P. Bird, Terahertz-frequency plasmonic-crystal instability in field-effect transistors with asymmetric gate arrays, *Scientific Reports* **14**, 11856 (2024).
- [37] J. M. Caridad, O. Castelló, S. M. L. Baptista, T. Taniguchi, K. Watanabe, H. G. Roskos, and J. A. Delgado-Notario, Room-temperature plasmon-assisted resonant thz detection in single-layer graphene transistors, *Nano Letters* **24**, 935 (2024).
- [38] A. Soltani, F. Kuschewski, M. Bonmann, A. Generalov, A. Vorobiev, F. Ludwig, M. M. Wiecha, D. Čibiraitė, F. Walla, S. Winnerl, S. C. Kehr, L. M. Eng, J. Stake, and H. G. Roskos, Direct nanoscopic observation of plasma waves in the channel of a graphene field-effect transistor, *Light: Science and Applications* **9**, 97 (2020).
- [39] M. S. Kushwaha, Plasmons and magnetoplasmons in semiconductor heterostructures, *Surface Science Report* **41**, 5 (2001).
- [40] I. V. Zagorodnev, A. A. Zabolotnykh, D. A. Rodionov, and V. A. Volkov, Two-dimensional plasmons in laterally confined 2d electron systems, *Nanomaterials* **13**, 975

- (2023).
- [41] V. L. Gurevich and Y. A. Firsov, A new oscillation mode of the longitudinal magnetoresistance of semiconductors, *Soviet Physics JETP* **20**, 489 (1965).
- [42] F. G. Bass and I. B. Levinson, Cyclotron-phonon resonance in semiconductors, *Soviet Physics JETP* **22**, 635 (1966).
- [43] F. M. Peeters and J. T. Devreese, Energy levels of two- and three-dimensional polarons in a magnetic field, *Phys. Rev. B* **31**, 3689 (1985).
- [44] P. Pfeffer and W. Zawadzki, Resonant and nonresonant polarons in semiconductors, *Phys. Rev. B* **37**, 2695 (1988).
- [45] P. Pfeffer and W. Zawadzki, Conduction electrons in gaas: Five-level $\mathbf{k}\cdot\mathbf{p}$ theory and polaron effects, *Phys. Rev. B* **41**, 1561 (1990).
- [46] C. Franchini, M. Reticcioli, M. Setvin, and U. Diebold, Polarons in materials, *Nature Reviews Materials* **6**, 560 (2021).
- [47] E. J. T. Devreese, F. Peeters, *Polarons and Excitons in Polar Semiconductors and Ionic Crystals* (Springer New York, NY, <https://doi.org/10.1007/978-1-4613-2693-9>, 1984).
- [48] S. D. Sarma, Polaron effective mass in gaas heterostructure, *Phys. Rev. B* **27**, 2590(R) (1983).
- [49] I. Grigelionis, M. Białek, M. Grynberg, M. Czapkiewicz, V. Kolkovsky, M. Wiater, T. Wojciechowski, J. Wróbel, T. Wojtowicz, N. Diakonova, W. Knap, and J. Łusakowski, Terahertz magneto-spectroscopy of a point contact based on CdTe/CdMgTe quantum well, *Journal of Nanophotonics* **9**, 093082 (2015).
- [50] I. Yokota, On the coupling between optical lattice vibrations and carrier plasma oscillations in polar semiconductors, *J. Phys. Soc. Japan* **16**, 2075 (1961).
- [51] B. B. Varga, Coupling of plasmons to polar phonons in degenerate semiconductors, *Phys. Rev.* **137**, A1896 (1965).
- [52] Y. C. Lee and N. Tzoar, Scattering of electromagnetic radiation by a nonequilibrium electron-phonon system, *Phys. Rev.* **140**, A396 (1965).
- [53] A. Mooradian and G. B. Wright, Observation of the interaction of plasmons with longitudinal optical phonons in gaas, *Phys. Rev. Lett.* **16**, 999 (1966).
- [54] P. Perlin, J. Camassel, W. Knap, T. Taliercio, J. C. Chervin, T. Suski, I. Grzegory, and S. Porowski, Investigation of longitudinal-optical phonon-plasmon coupled modes in highly conducting bulk gan, *Appl. Phys. Lett.* **67**, 2524 (1995).
- [55] A. Wysmolek, D. Plantier, M. Potemski, T. Ślupiański, and Z. R. Żytkiewicz, Coupled plasmon-LO-phonon modes at high-magnetic fields, *Phys. Rev. B* **74**, 165206 (2006).
- [56] S. S. Xiao, X. L. Zhu, B. H. Li, N. A. Mortensen, and N. Asger, Graphene-plasmon polaritons: From fundamental properties to potential applications, *Frontiers of Physics* **11**, 117801 (2016).
- [57] L. V. Kulik, I. V. Kukushkin, V. E. Kirpichev, K. von Klitzing, and K. Eberl, Interaction between intersubband bernstein modes and coupled plasmon-phonon modes, *Phys. Rev. B* **61**, 12717 (2000).
- [58] C. K. N. Patel and R. E. Slusher, Light Scattering from Electron Plasmas in a Magnetic Field, *Phys. Rev. Lett.* **21**, 1563 (1968).
- [59] N. Tzoar and E. N. Foo, Raman Scattering by Coupled Plasmon-Cyclotron-Harmonic Modes in Semiconducting Plasmas, *Phys. Rev.* **180**, 535 (1969).
- [60] F. A. Blum, Inelastic Light Scattering from Semiconductor Plasmas in a Magnetic Field, *Phys. Rev. B* **1**, 1125 (1970).
- [61] N. J. Horing and R. W. Danz, Bernstein modes and the quasiclassical model of the quantum plasma in magnetic field, *Journal of Physics C: Solid State Physics* **5**, 3245 (1972).
- [62] T. Kamimura, T. Wagner, and J. M. Dawson, Simulation study of Bernstein modes, *The Physics of Fluids* **21**, 1151 (1978).
- [63] R. R. Sharma, M. Salimullah, and V. K. Tripathi, Non-linear scattering of upper hybrid laser radiation by electron Bernstein modes in a plasma, *Phys. Rev. A* **21**, 942 (1980).
- [64] E. Batke, D. Heitmann, J. P. Kotthaus, and K. Ploog, Nonlocality in the Two-Dimensional Plasmon Dispersion, *Phys. Rev. Lett.* **54**, 2367 (1985).
- [65] V. Gudmundsson, A. Brataas, P. Grambow, B. Meurer, T. Kurth, and D. Heitmann, Bernstein modes in quantum wires and dots, *Phys. Rev. B* **51**, 17744 (1995).
- [66] D. E. Bangert, R. J. Stuart, H. P. Hughes, D. A. Ritchie, and J. E. F. Frost, Bernstein modes in grating-coupled 2DEGs, *Semiconductor Science and Technology* **11**, 352 (1996).
- [67] J. Lefebvre, J. Beerens, Y. Feng, Z. Wasilewski, J. Beauvais, and E. Lavallée, Bernstein modes in a laterally modulated two-dimensional electron gas, *Semiconductor Science and Technology* **13**, 169 (1998).
- [68] R. Krahné, M. Hochgräfe, C. Heyn, and D. Heitmann, Bernstein modes in density-modulated two-dimensional electron systems and quantum dots, *Phys. Rev. B* **61**, R16319(R) (2000).
- [69] S. Holland, C.-M. Hu, C. Heyn, and D. Heitmann, Bernstein modes in tunneling-coupled quantum wells, *Superlattices and Microstructures* **33**, 301 (2003).
- [70] A. A. Kapustin, S. I. Dorozhkin, and I. V. Kukushkin, Bernstein Modes in Two-Dimensional Electron Systems, *Journal of Surface Investigation: X-ray, Synchrotron and Neutron Techniques* **15**, 1133 (2021).
- [71] T. H. Stix, *The theory of plasma waves* (McGraw-Hill, New York City, 1962).
- [72] K. Nogajewski, Magnetoplasmon Excitations and Magnetotransport Properties of Two-Dimensional Electron Gas in GaN/AlGa_N Heterostructures, Ph. D. Thesis, University of Warsaw, <https://repozytorium.uw.edu.pl/entities/publication/4b2726c7-4f48-4ad1-9063-ad7bd114d172+> (2013).
- [73] D. A. Bandurin, E. Monch, K. Kapralov, I. Y. Phinney, K. Lindner, S. Liu, J. H. Edgar, I. A. Dmitriev, P. Jarillo-Herrero, D. Svintsov, and S. D. Ganichev, Cyclotron resonance overtones and near-field magnetoabsorption via terahertz Bernstein modes in graphene, *Nature Physics* **18**, 462 (2022).
- [74] I. Grigelionis, K. Nogajewski, G. Karczewski, T. Wojtowicz, M. Czapkiewicz, J. Wróbel, H. Boukari, H. Mariette, and J. Łusakowski, Magnetoplasmons in high electron mobility CdTe/CdMgTe quantum wells, *Phys. Rev. B* **91**, 075424 (2015).
- [75] M. A. Zudov, R. R. Du, J. A. Simmons, and J. L. Reno, Shubnikov-de haas-like oscillations in millimeter wave photoconductivity in a high-mobility two-dimensional

- electron gas, *Phys. Rev. B* **64**, 201311(R) (2001).
- [76] Y. Dai, R. R. Du, L. N. Pfeiffer, and K. W. West, Observation of a cyclotron harmonic spike in microwave-induced resistances in ultraclean GaAs/AlGaAs quantum wells, *Phys. Rev. Lett.* **105**, 246802 (2010).
- [77] M. Białek, J. Łusakowski, M. Czapkiewicz, J. Wróbel, and V. Umansky, Photoresponse of a two-dimensional electron gas at the second harmonic of the cyclotron resonance, *Phys. Rev. B* **91**, 045437 (2015).
- [78] M. L. Savchenko, A. Shuvaev, I. A. Dmitriev, A. A. Bykov, A. K. Bakarov, Z. D. Kvon, and A. Pimenov, High harmonics of the cyclotron resonance in microwave transmission of a high-mobility two-dimensional electron system, *Phys. Rev. Research* **3**, L12013 (2021).
- [79] S. A. Mikhailov, Theory of microwave-induced zero-resistance states in two-dimensional electron systems, *Phys. Rev. B* **83**, 155303 (2011).
- [80] V. A. Volkov and A. A. Zabolotnykh, Bernstein modes and giant microwave response of a two-dimensional electron system, *Phys. Rev. B* **89**, 121410 (2014).
- [81] R. J. Nicholas, M. Watts, D. F. Howell, F. M. Peeters, X.-G. Wu, J. T. Devreese, L. van Bockstal, F. Herlach, C. J. G. M. Langerak, J. Singleton, and A. Chevy, Cyclotron resonance of both magneto-polaron branches for polar and neutral optical phonon coupling in the layer compound InSe, *Phys. Rev. B* **45**, 12144 (1992).
- [82] Y. Imanaka, T. Takamasu, G. Kido, G. Karczewski, T. Wojtowicz, and J. Kossut, Cyclotron resonance in high mobility CdTe/CdMgTe 2D electron system in the integer quantum Hall regime, *Physica B: Condensed Matter* **256 - 258**, 457 (1998).
- [83] G. Karczewski, T. Wojtowicz, Y. Wang, X. Wu, and F. Peeters, Electron effective mass and resonant polaron effect in CdTe/CdMgTe quantum wells, *Phys. Status Solidi B* **229**, 597 (2002).
- [84] B. K. Ridley, *Electrons and Phonons in Semiconductor Multilayers* **26**, 7867 (1982). (Cambridge University Press, ISBN-13 978-1107424579, 2nd Ed., 2014).
- [85] D. Liu, J. Chen, D. Wang, L. Wu, and D. Wang, Enhanced surface optical phonon in cdte thin film observed by raman scattering, *Appl. Phys. Lett.* **113**, 061604 (2018).
- [86] A. M. de Paula, L. C. Barbosa, C. H. B. Cruz, O. L. Alves, J. A. Sanjurjo, and C. L. Cesar, Quantum confinement effects on the optical phonons of cdte quantum dots, *Superlattices and Microstructures* **23**, 1103 (1998).
- [87] W. Solarska, K. Karpierz, M. Zaremba, F. L. Mardelé, I. Mohelsky, A. Siemaszko, M. Grymuza, L. Kipcza, N. Zawadzka, M. R. Molas, E. Imos, Z. Adamus, T. Słupiński, T. Wojtowicz, M. Orlita, A. Babiński, and J. Łusakowski, Magnetophotoluminescence of modulation-doped cdte multiple quantum wells, *ACS Omega* **8**, 40801 (2023).
- [88] D. Strauch, Cdte: phonon frequencies, in *New Data and Updates for several III-V (including mixed crystals)* edited by U. Rossler (Springer Berlin Heidelberg, Berlin, Heidelberg, 2012) pp. 152–153.
- [89] D. V. Fateev, V. V. Popov, and M. S. Shur, Transformation of the plasmon spectrum in a grating-gate transistor structure with spatially modulated two-dimensional electron channel, *Semiconductors+* **44**, 1406 (2010).
- [90] A. L. Fetter, Electrodynamics of a layered electron gas. i. single layer, *Annals of Physics* **81**, 367 (1973).
- [91] A. L. Fetter, Electrodynamics of a layered electron gas. ii. periodic array, *Annals of Physics* **88**, 1 (1974).
- [92] S. D. Sarma and J. J. Quinn, Collective excitations in semiconductor superlattices, *Phys. Rev. B* **25**, 7603 (1982).
- [93] G. F. Guliani and J. J. Quinn, Charge-density excitations at the surface of a semiconductor superlattice: A new type of surface polariton, *Phys. Rev. Lett.* **51**, 919 (1983).
- [94] J. J. Jain and P. B. Allen, Plasmons in layered films, *Phys. Rev. Lett.* **54**, 2437 (1985).
- [95] V. Y. Aleshkin and A. A. Dubinov, Plasmon absorption reduction in multiple quantum well structures, *Applied Optics* **61**, 3583 (2022).
- [96] D. Olego, A. Pinczuk, A. C. Gossard, and W. Wiegmann, Plasma dispersion in a layered electron gas: A determination in gaas-(alga)as heterostructures, *Phys. Rev. B* **26**, 7867 (1982).
- [97] G. Fasol, N. Mestres, H. P. Huges, A. Fisher, and K. Ploog, Raman scattering by coupled-layer plasmons and in-plane two-dimensional single-particle excitations in multi-quantum-well structures, *Phys. Rev. Lett.* **56**, 2517 (1986).